Polymer Chemistry

Metal-Organic Insertion Light Initiated Radical (MILRad) Polymerization: Photo-initiated Radical Polymerization of Vinyl Polar Monomers with Various Palladium Diimine Catalysts

Journal:	*Polymer Chemistry*
Manuscript ID	PY-COM-10-2018-001556.R1
Article Type:	Communication. Paper
Date Submitted by the Author:	05-Dec-2018

Complete List of Authors:	Keyes Jr., Anthony; University of Houston Dau, Huong; University of Houston Basbug Alhan, Hatice; University of Houston Ha, Uyen; University of Houston Ordonez, Estela; University of Houston, Department of Chemistry Jones, Glen; University of Houston, Department of Chemistry Liu, Yu-Sheng; University of Houston, Department of Chemistry Tsogtgerel, Enkhjargal ; University of Houston, Department of Chemistry Loftin, Breyinn; University of Houston, Department of Chemistry Wen, Zhili ; University of Houston, Department of Chemistry Wu, Judy; University of Houston, Department of Chemistry Beezer, Dain; University of Houston, Department of Chemistry Harth, Eva; University of Houston, Department of Chemistry ; University of Houston, Chemistry

Polymer Chemistry

ARTICLE

Metal-Organic Insertion Light Initiated Radical (MILRad) Polymerization: Photo-initiated Radical Polymerization of Vinyl Polar Monomers with Various Palladium Diimine Catalysts

Received 00th January 20xx,
Accepted 00th January 20xx

DOI: 10.1039/x0xx00000x

www.rsc.org/

Anthony Keyes, Huong Dau, Hatice E. Basbug Alhan, Uyen Ha, Estela Ordonez, Glen R. Jones, Yu-Sheng Liu, Enkhjargal Tsogtgerel, Breyinn Loftin, Zhili Wen, Judy I. Wu*, Dain B. Beezer* and Eva Harth*

Controlled insertion polymerization with organometallic catalysts has served as the foundation for the production of polymers with precise control, and have become ubiquitous in industrial settings. We investigate the photoinitiated radical polymerization pathway of metal-organic insertion light initiated radical (MILRad) polymerization towards its ability to polymerize a variety of vinyl polar functional monomers. A series of Pd-diimine catalysts were synthesized and tested in their ability to produce homopolymers of polar vinyl monomers such as acrylates, methacrylates, acrylamides, styrene, vinyl ethers and vinyl acetate in the dark and under photoinitation at 460 nm. Acrylates and methacrylates were found to polymerize in the light but not in the dark against all catayst tested. Acrylamides displayed a stronger dependence on the catayst structure when polymerized in the light. Other monomer families such as styrene, vinyl ether and vinyl acetate, showed either a limited selectivity and conversions, a prefered cationic polymerization pathway or no reaction. Computational studies were conducted to examine the excited states of the catalysts and the energies associated with those transitions. Results of density functional theory (DFT) and time-dependent DFT (TD-DFT) studies indicate low energy metal-to-ligand charge transfer (MLCT) transitions from Pd-Me σ-bonding into ligand π orbitals leads to reduction of the Pd-Me σ-bond. In this work, we illustrate a dormant radical pathway accessible by all diimine cationic Pd(II) catalysts and will expand the scope of MILRad polymerization for the preparation of block copolymers.

Introduction

The development of complex metal-organic catalysts which coordinate and polymerize electron rich α-olefins via an insertion pathway[1-9] with high control over molecular weight and branching has been an ever present topic of exploration to this day and has resulted in materials that became ubiquitous in everyday life, commonly known as plastics.[10] The insertion polymerization that governs these catalysts has largely excluded the polymerization of acrylic monomers, a class which are also highly desired and well known for their conventional radical polymerization and reversible-deactivation radical polymerization (RDRP) processes.[11-16] Both polymerization methodologies, insertion and radical polymerization, have generally been tailored towards the characteristics of two monomer classes, non-polar olefins and functional polar monomers. Efforts in copolymerization were focused on either increasing functional group tolerance of polar vinyl monomers in the insertion polymerization pathway[8, 9, 17-19] or to employ alternative radical polymerizations with non-polar olefins.[20-27] Both approaches have led to some success with the combination of monomers in polar and non-polar character, but the challenge still remains to find a selective platform covering a wide range of functionality and polarity.

Brookhart-type cationic α-diimine palladium catalysts[28-31] were the first late transition metal-organic catalysts which produced polymers of ethylene and α-olefins with high molecular weight and various degrees of branching, resulting in control of the polymer microstructure due to its unique chain walking mechanism. The facile synthesis and the functional group tolerance lead to intense investigations to not only produce non-polar macromolecular architectures but also probe the copolymerization with polar vinyl monomers to access highly desired functional polyethylenes[32]. Although a high activity through the insertion pathway was observed with vinyl triethoxysilane[33], it is regarded as an exception as most other polar vinyl monomers insert only once, incapable of further polar monomer incorporation due to isomerization which leads to strong chelate formation inhibiting the chain growth polymerization. However, ethylene coordination can lead to opening of the chelate, followed by subsequent insertion and continued olefin polymerization where single polar monomer incorporations are restricted to polymer chain-end groups.[30, 34, 35] Therefore, the homopolymerization of polar monomers through insertion polymerization remains ineffective for the synthesis of block copolymers. Efforts to

[a] Department of Chemistry, Center of Excellence in Polymer Chemistry (CEPC), University of Houston, 3585 Cullen Boulevard, Houston, Texas 77030, United States. email: harth@uh.edu; dbbeezer@uh.edu; jiwu@central.uh.edu
Electronic Supplementary Information (ESI) available: data and experimental details
See DOI: 10.1039/x0xx00000x

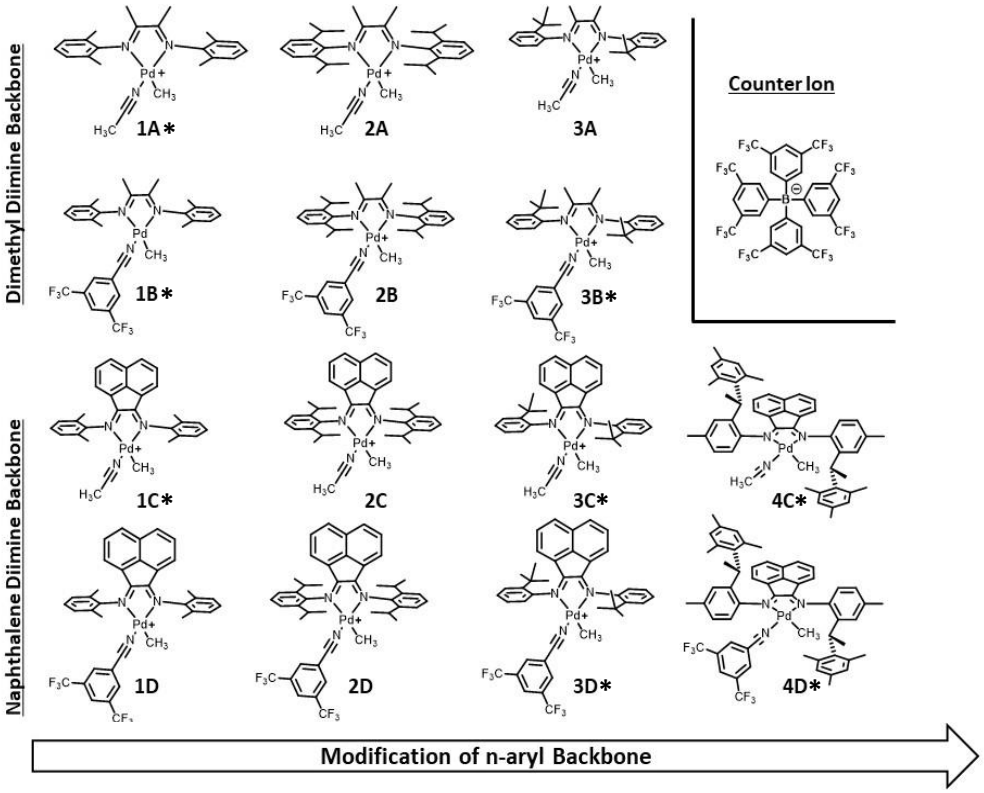

Scheme 1. Complete list of cationic palladium diimine catalysts tested in this study, including previously synthesized and novel catalysts. *Novel derivatives.

perform radical polymerizations with palladium diimine catalysts have been made possible affording the homopolymerization of acrylates.[36-38] This has represented a step forward, but these approaches still proved incapable of synthesizing block copolymers until the discovery of MILRad polymerization, in which a Pd-diimine catalyst can selectively perform insertion and photoinitiated radical polymerizations.[39] This platform allowed the catalyst to initiate a radical polymerization following insertion polymerization yielding block copolymers of hexene and methyl acrylate. This technique sparked interest towards the polymerization of a wider range of polar vinyl monomers, which until now had not been compatible with diimine Pd-catalysts. It is also equally important to test if changes in the structure of diimine Pd-catalysts have an impact on monomer scope, affect the control over the polymerization, or if selectivity could be afforded through ligand design.

In this work, we explore the photoinitiated radical polymerization pathway of MILRad polymerization for commercially relevant polar vinyl monomers with multiple palladium diimine catalysts. Substitution of ancillary ligands and n-aryl functionalization produced a range of MILRad candidates that were tested with several monomer classes to show the versatility of this technique. In these efforts, we demonstrate the expansion of monomers that were previously inaccessible using diimine Pd-catalysts.[10, 30, 35, 40-42] Computational studies were performed to give insight into the electronic transitions of all catalysts and understand the necessary components impacting radical polymerization. Excited states from TD-DFT calculations identified MLCT transitions which show a transfer from the metal-carbon σ-bond to the ligand's π-system which promotes the homolysis of the metal-carbon bond generating radicals, indicating that the diimine ligand is crucial for radical polymerization and transitions arise from the excitation in the visible light spectrum. This work establishes polar vinyl monomers that, in combination with non-polar monomers, meet the criteria for MILRad polymerization to produce a series of novel specialized block copolymers with potential applications as functionalized thermoplastics and compatibilizers.

Results and discussion

We previously established MILRad polymerization[39] as a synthetic technique for light triggered radical polymerization with a palladium diimine catalyst, an orthogonal route to insertion polymerization. This novel polymerization technique enables the preparation of block copolymers with polar and non-polar segments in a sequential and one-pot pathway from monomers that were previously inaccessible using a single catalyst. The aim of this work was to explore if this technique could be expanded to other diimine catalysts, explore the polar vinyl monomer scope of the photoinitated polymerization process, and investigate how changes to catalysts structure influence the radical polymerization. We selected in total 14 catalysts, of which 1D, 2A-D, 3A[30, 40] are well studied for insertion polymerization while synthesizing new derivatives, 1A-C, 3B-D, and 4C-D to explore their radical polymerization

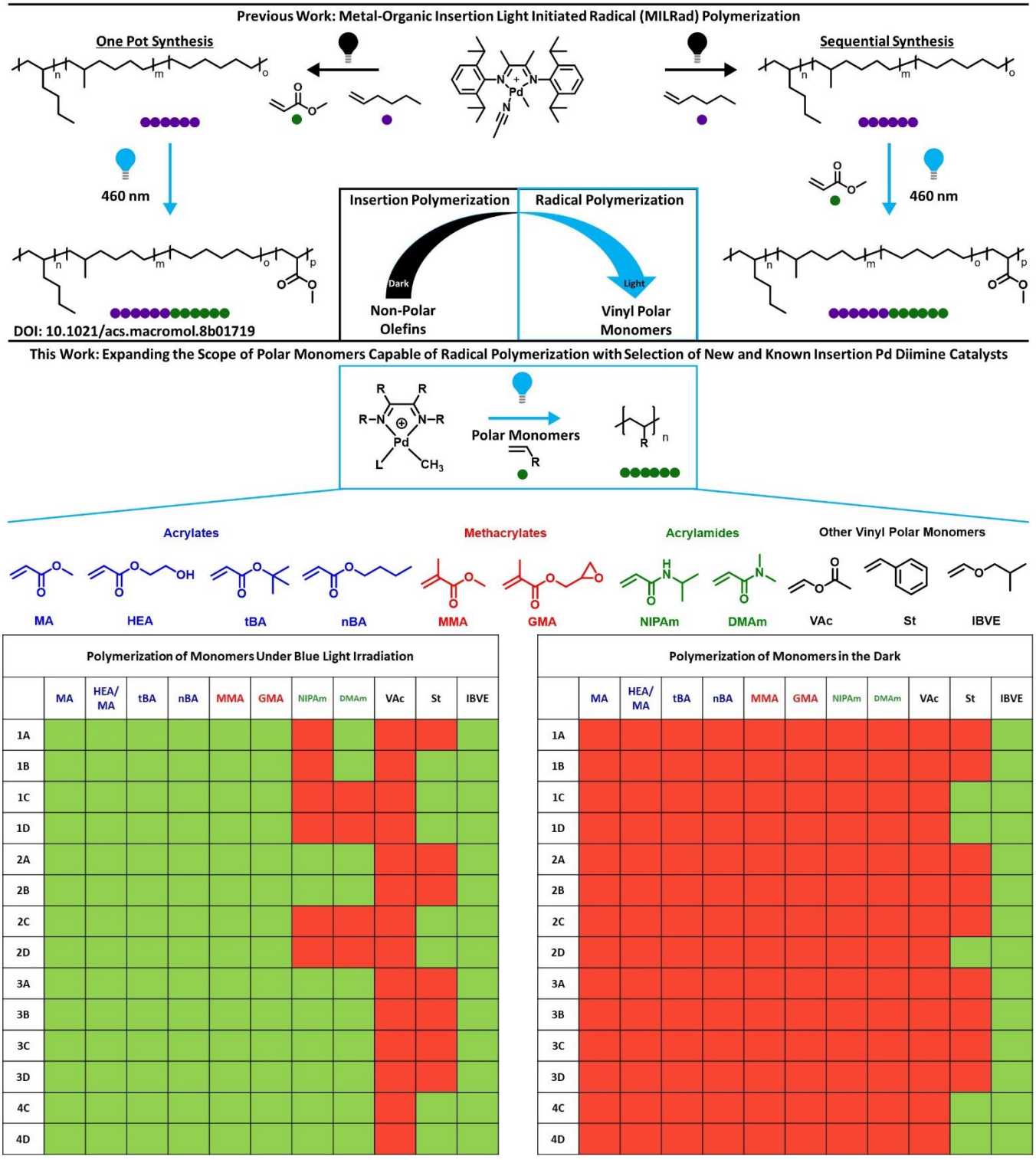

Scheme 2. (Top) Outline for the synthesis of block copolymers via MILRad Polymerization. (Bottom) Selection of polar vinyl monomers for radical polymerization via blue light irradiation and corresponding heatmaps for successful polymerization (green) and unsuccessful polymerization (red).

capabilities while varying the diimine backbone, ancillary ligands and n-aryl substituents (Scheme 1). Furthermore, a series of functionalized polar vinyl monomers (Scheme 2) were tested against all catalysts affording over 300 polymerization reactions. Through this endeavor, we lay the groundwork for MILRad polymerization with a toolkit of monomers that are capable of polymerizing in a completely orthogonal manner. From this work, a range of new polymer architectures can be designed employing the newly accessed monomers.

Acrylate Screening. Methyl acrylate was first tested with all the catalysts synthesized (Scheme 1) and showed polymer formation in all cases of light irradiation (Table S1). All catalysts were capable of performing radical polymerization when irradiated with light. Catalyst 1D exhibited a more controlled

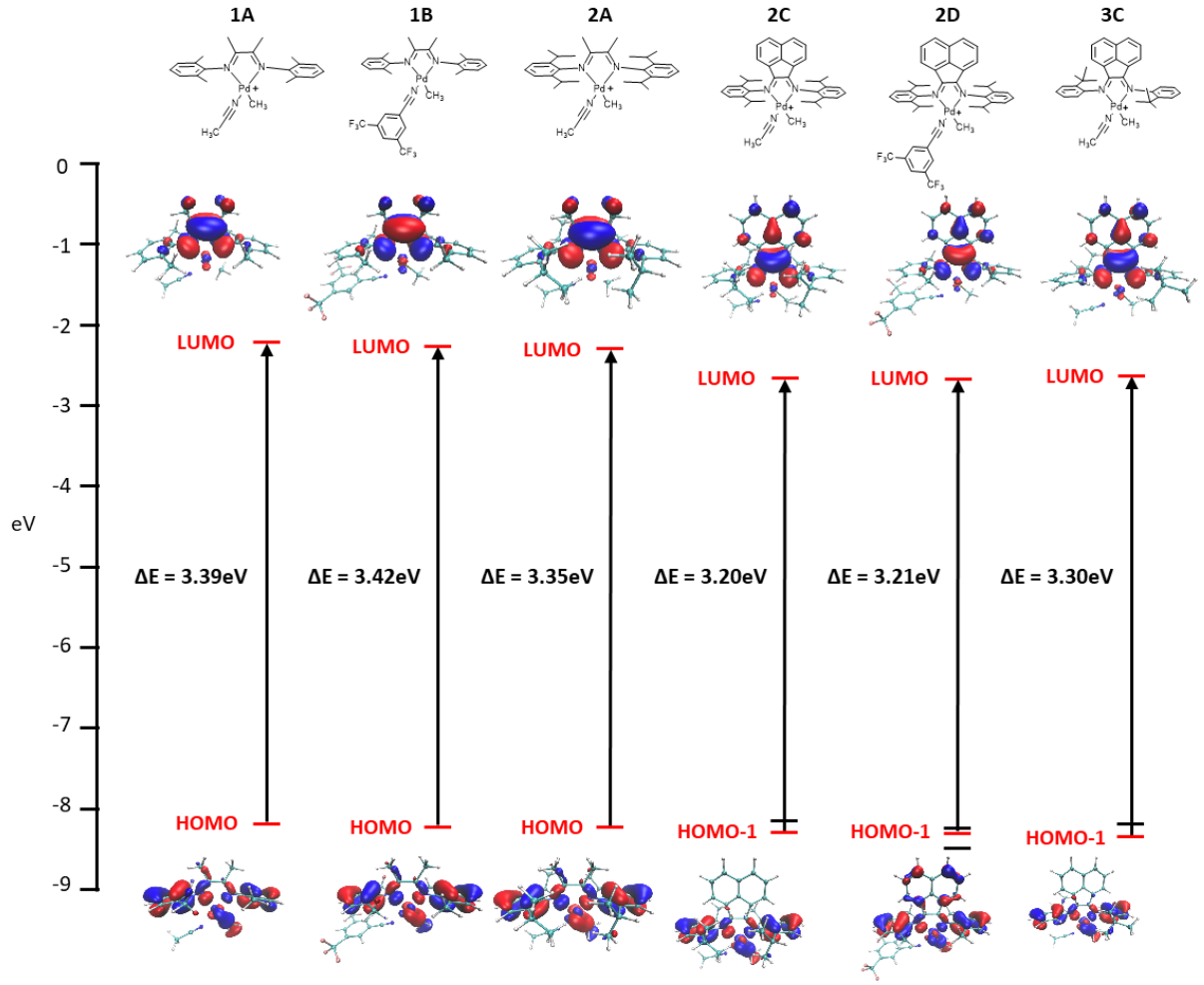

Scheme 3. Calculated HOMO/LUMO energy diagram of complexes 1A, 1B, 2A, 2C, 2D, and 3C. The most prominent MOs involved with transitions under the low energy band and their diagrams are shown.

radical polymerization for MA, with an improved dispersity of 1.76 in contrast to 2A, the catalyst of previous studies (Table 1, Table S1). No polymerization was witnessed in the dark for all catalysts, and this would serve as an orthogonal process for future block copolymer development. 2-hydroxyethyl acrylate (HEA) was copolymerized with methyl acrylate in a 1:4 molar ratio, establishing the ability to install functionalities, i.e. hydroxyl units suitable for post functionalization when MILRad polymerization would be performed. All catalysts copolymerized the monomers in the light, yielding different compositions, and no polymerization was seen in the dark (Table S3, S4). Catalyst 3C exhibited the best control (Table 1, Table S3). Although HEA was copolymerized as a minority monomer component in the reactions, it consistently showed a higher conversion compared to methyl acrylate and the difference in monomer reactivity ratios agrees with literature reports.[43] Tert-butyl acrylate (tBA) polymerized with all catalysts in the light, and no conversion was seen in the dark and produced the largest range in molecular weights (44-1224 kg/mol), dispersities (1.78-5.83), and conversions (14-86%). Catalysts 2C exhibited the best control in this set of experiments, with a dispersity of 2.16 and reasonable molecular weight targeting and conversion (Table 1, Table S5). In contrast, n-butyl acrylate, as expected, showed much higher control in molecular weight targeting, dispersity, and conversions comparable to methyl acrylate and catalyst 3A revealed the best control (Table 1, Table S7).

Methacrylate Screening. Methacrylates showed slower reaction rates compared to acrylates. The conversion for all reactions of MMA were less than that of the MA, with a difference of 27% and 78% respectively. This is consistent with the lower K_p of methacrylates (2 magnitudes lower) compared to acrylates.[44] However, it was observed that MMA can reach high conversions of 70% when reacted for 3 days. MMA did not polymerize in the dark with any of the catalysts, and dispersities never exceeded 2.0 with catalyst 2A exhibiting the best control (Table 1, Table S9). Glycidyl methacrylate (GMA) showed higher rates of reaction and similar control in polymerization compared to MMA. The higher reactivity of GMA is attributed to the higher propagation rate typically seen in conventional radical polymerizations (K_p (GMA) = 1600 vs K_p (MMA) 820 $M^{-1}s^{-1}$).[44] All reactions polymerized in the light, and not the dark. No opening of the epoxide ring was observed for the majority of the catalysts, yet catalysts 2A-D showed bimodal GPC traces in part to opening of the epoxide. Catalyst 3B was selected as the most appropriate catalyst for GMA (Table 1, Table S11). The

Table 1. Polymerization of Highlighted Monomer and Catalyst Pairs

Monomer	Catalyst	Molar Ratio[a] [M]:[Cat]	Reaction Time[b] (Hours)	$M_{n,\,GPC}$[c] kg/mol	$M_{w,\,GPC}$[c] kg/mol	$Đ$[c] (M_w/M_n)	α[d] (%)	DP[e]
MA	1D	1162:1	16	92	162	1.76	63	732
HEA-MA[f]	3C	1108:1	16	168	295	1.75	57	569
tBA	2C	780:1	16	138	297	2.16	49	382
nBA	3A	780:1	16	120	198	1.65	63	491
MMA	2A	999:1	24	87	151	1.74	27	270
GMA	3B	704:1	24	95	172	1.81	74	521
NIPAm	3C	1009:1	24	187	385	2.06	19	167
DMAm	1A	880:1	24	257	414	1.65	29	293
VAc	---	1162:1	16	---	---	---	---	---
St	4D	960:1	24	35	67	1.91	26	250
IBVE	1B	999:1	16	18	35	2.02	99	989

Table 1.[a]Catalyst to monomer ratio. [b]Theoretical molecular weight for all reactions targeted for 100 kg/mol. [c]Molecular weight and polydispersity index (M_w/M_n) were determined by GPC analysis calibrated with polymethyl methacrylate standards. [d]Monomer conversion was determined by ^{1}H NMR spectroscopy. [e]Degree of polymerization. [f]Molecular weight targeted with 20 mol% of HEA.

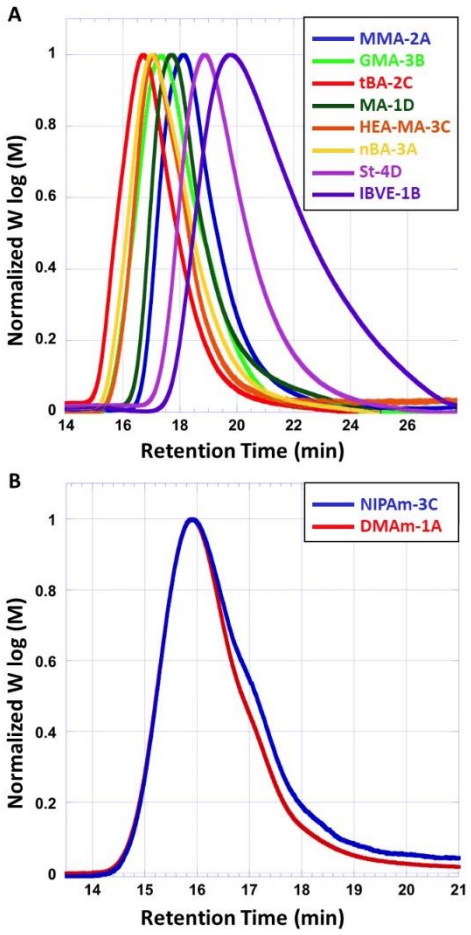

Scheme 4. GPC traces shown on the right for monomer and catalyst pairs highlighted in Table 1. (**A**) Polymer GPC traces for vinyl polar monomers were obtained from samples (precipitated) measured in THF at 40°C using polymethyl methacrylate standards. (**B**) Polymer GPC traces for acrylamides were obtained from samples (precipitated) measured in DMF at 60°C using polymethyl methacrylate standards.

ability to maintain the integrity of the epoxide during a radical polymerization is of great value for the development of complex materials, and will be subject of further studies.

Acrylamide Screening. For dimethyl acrylamide (DMAm) no catalysts formed polymers in the dark. In the light, catalysts 1C, 1D, 2C, 2D, and 3D showed no polymerization of DMAm. For n-isopropyl acrylamide (NIPAm) no polymers formed in the dark. Similar to DMAm, catalysts 1C, 1D, 2C, and 2D did not polymerize in addition to 1A and 1B. Polymerization of acrylamides with Pd-catalysts has been proven to be very challenging via an insertion polymerization pathway.[10] Previous studies have shown that nitrogen containing monomers can promote the decomposition of the Pd-diimine catalyst through strong interaction of Pd with the nitrogen atom via a sigma binding mode.[45-47] The observed differences in reactivity between NIPAm and DMAm can be attributed to the preference for sigma binding of the secondary nitrogen atom in NIPAm compared to the tertiary nitrogen atom present in DMAm. Furthermore, the increased steric interactions induced by the bulky backbone of the diimine ligands in catalyst 1C, 1D, 2C, and 2D seems to encourage preferential binding of the nitrogen atom over the alkene. We envision this is a limiting factor in the endeavored radical polymerization pathway but it is not fully understood and is currently under investigation.

Vinyl Acetate, Styrene and Vinyl Ether Screening. For vinyl acetate (VAc), there was no polymerization observed in the dark nor the light for all catalysts tested (Table 1, Table S17). Prior investigations into the reactivity of vinyl acetate with cationic Pd-diimine catalyst revealed that the relative energies associated with the 2,1 insertion of the vinyl acetate into the Pd-Me bond was similar to that of MA (18.6 and 15.1 kcal mol^{-1} respectively), which would suggest that like MA, vinyl acetate inserted into the Pd-Me bond of the catalyst. However, 2,1 insertion of vinyl acetate resulted in the formation of a five member chelate complex, with a relative energy (-15.6 kcal mol^{-1}) that is significantly higher than that of the four member chelate complex formed by MA (-6.9 kcal mol^{-1}).[48] The higher stability of chelate complex formed by vinyl acetate prevents the homolysis of the Pd-alkyl bond and is expected to be the inhibiting factor in the radical polymerization via blue light irradiation. Other studies have shown that weak metal-carbon bonds such as those found in many cobalt-alkyl complexes, are more susceptible to bond homolysis and have proven successful for the polymerization of less activated monomers such as vinyl acetate.[49] These reports highlight the importance of metal-carbon bond strength and chelate complex binding energies on radical polymerizations mediated by an organometallic catalyst.

For styrene (St), two catalysts exhibited selective polymerization in the light and not in the dark (1B and 2C) with low conversions (Table 1, Table S19). However, five other catalysts yielded polymers both in the light and the dark. This could be attributed to the existence of both a radical and

cationic pathway. The insertion of styrene into the Pd-Me bond favors the formation of a stable π-benzyl complex which then leads to chain termination via β-hydride elimination thereby inhibiting the insertion polymerization of styrene.[10, 50, 51] Consequently, the observed polymerization activity displayed by the Pd-diimine complexes can be attributed to a radical or cationic mechanism and is the subject of current investigation in our lab. Isobutyl vinyl ether (IBVE) was polymerized to high conversions with all catalysts in the light and in the dark (Table 1, S21). Cationic Pd-diimine catalysts have been reported to polymerize IBVE preferentially in a cationic manner, with the mechanism relying on trace amounts of water, which is present even after rigorous purification of reagents. A generated palladium aqua species affords a proton transfer to the IBVE forming the oxonium intermediate which undergoes a chain growth polymerization aided by the cationic stability of IBVE.[52, 53] Neutral phosphine-sulfonate palladium catalysts have overcome the cationic polymerization promoting the insertion polymerization of vinyl ethers.[54] Access all these polymerization pathways is expected to create and even more robust catalytic toolbox to compliment radical and insertion techniques, and will be explored further in future work.

In summary, this study revealed that acrylate, methacrylate and acrylamide monomers all display complete selectivity to polymerize in the light under a radical pathway. This selectivity is desired for future development of block copolymers, where insertion and radical polymerization can be separated from one another using light as a switchable stimulus. For the non-acrylic monomers, a selective radical pathway was not observed, suggesting that the acrylic motif plays a crucial role in the radical polymerization process.

DFT and TD-DFT Calculations. Density functional theory (DFT) calculations were carried out at the M06-2X/6-31+G(d,p) level to identify key features of the studied catalysts that contribute to radical polymerizations.[55-58] Structurally similar catalysts were compared to study the effects of ligand substitution on the HOMO-LUMO gaps and electronic transitions of catalysts. Pairs of catalysts were selected to investigate changes in the ancillary ligands (1A and 1B), diimine backbone (2A and 2C), increased steric substitution (2C and 3C) and a combination of all three (1A and 2D). Vibrational frequency analyses verified the nature of the stationary points (see details in the ESI). Vertical excitation energies were computed using time-dependent density functional theory (TD-DFT) at the same level of theory. Molecular orbitals were visualized using VMD[59] and all calculations were performed employing Gaussian 09[30].

The molecular orbital (MO) energy diagram, shown in Scheme 3, displays the compositions of the lowest occupied MOs and the LUMO of 1A, 1B, 2A, 2C, 2D, and 3C and displays transitions for all six catalysts from the HOMO or HOMO-1 orbitals and LUMO. All catalysts consistently exhibit loss of electron density in the metal-carbon bond and gain of electron density in the ligand π systems. This transition indicates a MLCT that is constantly found in all catalysts explored. Catalysts with dimethyl backbones (1A, 1B, and 2A) exhibited HOMO→LUMO transitions of 366, 363, and 370 nm respectively (Scheme 3). These calculated transitions correlate to bands in the UV-Vis spectrum for all catalysts explored to polymerize the monomers of this study. For catalysts with naphthalene backbones (2C, 2D, and 3C), HOMO-1→LUMO transitions of 388, 386, and 376 nm were exhibited respectively (Scheme 3), and these transitions are also in agreement with the bands observed in the UV-Vis spectrum. The HOMO's of all catalysts lie at similar energy levels, however, the LUMO's of catalysts 2C, 2D, and 3C all have lower energy orbitals compared to catalysts 1A, 1B, and 2A that show a decrease of ~0.2 eV (4-5 kcal/mol). The LUMO lowering seen in these catalysts is attributed to the conjugated ring systems in the naphthalene backbone compared with the dimethyl backbone present in catalysts 1A, 1B, and 2A and is expected to stabilize the LUMO.

In our prior studies, we discovered that irradiation with blue light led to the loss of the methyl group in the 2A Pd-diimine catalyst and was attributed to the homolysis of the metal-carbon bond.[39, 60, 61] The MLCT transitions observed in this work illustrate a shift in electron density from the metal-carbon σ-bond to the ligand π frame, which is expected to decrease the strength of the metal-carbon bond, and promote the radical polymerization. The calculated energies from 360-380nm further support that MLCT transitions leads to photolabile metal-carbon bonds which are responsible for the radical polymerization in these photocatalytic systems. In light of the identification of MLCT transitions, we discovered that systematic changes in the catalyst do not have a significant change in the HOMO LUMO gaps for the catalysts. This observation suggests that differences in MLCT transitions are not responsible for unsuccessful polymerization of acrylamides with catalysts 1A-D and 2C-D.

Taken together, the results of the theoretical calculations qualitatively support the hypotheses that guided our catalyst selection for the screening process. It is evident that low energy MLCT transitions arising from MOs with metal-carbon bonding character to MOs associated with the π-frame of the ligand could lead to scission of the Pd-Me bond in the present catalysts (1A, 1B, 2A, 2C, 2D, and 3C) upon exposure to visible light. The results of the present work indicate that multiple Pd catalysts are capable of MILRad polymerization, which is understood to access the radical pathway through a MLCT transition. More rigorous theoretical studies to establish the details of the mechanism of radical generation arising from the MLCT transition(s) and the differences in monomer reactivity's are currently under way.

Conclusions

In conclusion, we demonstrate that a radical polymerization can be initiated from a wide range of cationic palladium diimine catalysts with various ancillary ligands, diimine backbone structures, and aryl substituents by irradiation with blue light. The polymerization of (meth)acrylates, acrylamides, styrene, vinyl acetate and isobutyl vinyl ether were attempted with all catalyst complexes. Importantly, polymerization of acrylates, methacrylates, and acrylamides is reported to proceed only in the presence of light. Results of the theoretical calculations reveal MLCT transitions that occur between a metal-carbon

bond and diimine backbone, which are hypothesized to account for the ability to initiate a radical polymerization. The HOMO-LUMO gaps exhibit a negligible difference between complexes, suggesting that the ligand structure of catalysts does not significantly influence the photoinitiation process. These results broaden the scope of the recently reported MILRad polymerization protocol, and could allow for facile, one-pot synthesis of amphiphilic block copolymers of olefins with various polar vinyl monomers.

Conflicts of interest

There are no conflicts to declare.

Acknowledgements

The authors thank the Robert A. Welch Foundation for generous support of this research (#H-E-0041) through the Center of Excellence for Polymer Research. A.K. acknowledges the National Science Foundation (NSF) Graduate Research Fellowship Program (GRFP), The University of Houston Presidential Fellowship, and the Center of Excellence in Polymer Chemistry Fellowship. B.L. acknowledges the National Science Foundation (NSF) Graduate Research Fellowship Program (GRFP). J.I.W. thanks the NSF for funding support (CHE-1751370). All computations were performed through resources of the uHPC cluster managed by the University of Houston and acquired through NSF support (MRI-1531814).

Notes and references

1. D. Takeuchi, *Dalton Trans.*, 2010, **39**, 311-328.
2. H. Zou, F. M. Zhu, Q. Wu, J. Y. Ai and S. A. Lin, *J. Polym. Sci., Part A: Polym. Chem.*, 2005, **43**, 1325-1330.
3. B. K. Bahuleyan, G. W. Son, D. W. Park, C. S. Ha and I. Kim, *J. Polym. Sci., Part A: Polym. Chem.*, 2008, **46**, 1066-1082.
4. J. Merna, Z. Host'alek, J. Peleska and J. Roda, *Polymer*, 2009, **50**, 5016-5023.
5. C. S. Popeney and Z. B. Guan, *Macromolecules*, 2010, **43**, 4091-4097.
6. J. L. Rhinehart, L. A. Brown and B. K. Long, *J. Am. Chem. Soc.*, 2013, **135**, 16316-16319.
7. K. F. Song, W. H. Yang, B. X. Li, Q. B. Liu, C. Redshaw, Y. S. Li and W. H. Sun, *Dalton Trans.*, 2013, **42**, 9166-9175.
8. K. E. Allen, J. Campos, O. Daugulis and M. Brookhart, *ACS Catal.*, 2015, **5**, 456-464.
9. S. Y. Dai, X. L. Sui and C. L. Chen, *Angew Chem Int Edit*, 2015, **54**, 9948-9953.
10. S. D. Ittel, L. K. Johnson and M. Brookhart, *Chem. Rev.*, 2000, **100**, 1169-1203.
11. K. Matyjaszewski and J. H. Xia, *Chem. Rev.*, 2001, **101**, 2921-2990.
12. C. J. Hawker, A. W. Bosman and E. Harth, *Chem. Rev.*, 2001, **101**, 3661-3688.
13. C. Boyer, V. Bulmus, T. P. Davis, V. Ladmiral, J. Q. Liu and S. Perrier, *Chem. Rev.*, 2009, **109**, 5402-5436.
14. J. Yeow, R. Chapman, A. J. Gormley and C. Boyer, *Chem. Soc. Rev.*, 2018, **47**, 4357-4387.
15. M. Chen, M. J. Zhong and J. A. Johnson, *Chem. Rev.*, 2016, **116**, 10167-10211.
16. C. Boyer, N. A. Corrigan, K. Jung, D. Nguyen, T. K. Nguyen, N. N. M. Adnan, S. Oliver, S. Shanmugam and J. Yeow, *Chem. Rev.*, 2016, **116**, 1803-1949.
17. S. Dai, S. Zhou, W. Zhang and C. Chen, *Macromolecules*, 2016, **49**, 8855-8862.
18. S. Ramakrishnan, E. Berluche and T. C. Chung, *Macromolecules*, 1990, **23**, 378-382.
19. J. M. Kaiser and B. K. Long, *Coord. Chem. Rev.*, 2018, **372**, 141-152.
20. A. Kermagoret, A. Debuigne, C. Jérôme and C. Detrembleur, *Nat. Chem.*, 2014, **6**, 179-187.
21. E. Mishima, T. Tamura and S. Yamago, *Macromolecules*, 2012, **45**, 8998-9003.
22. R. Venkatesh and B. Klumperman, *Macromolecules*, 2004, **37**, 1226-1233.
23. R. Venkatesh, S. Harrisson, D. M. Haddleton and B. Klumperman, *Macromolecules*, 2004, **37**, 4406-4416.
24. R. Venkatesh, F. Vergouwen and B. Klumperman, *Macromol. Chem. Phys.*, 2005, **206**, 547-552.
25. S. Liu, B. Gu, H. A. Rowlands and A. Sen, *Macromolecules*, 2004, **37**, 7924-7929.
26. S. Liu, S. Elyashiv and A. Sen, *J. Am. Chem. Soc.*, 2001, **123**, 12738-12739.
27. D. Benoit, E. Harth, P. Fox, R. M. Waymouth and C. J. Hawker, *Macromolecules*, 2000, **33**, 363-370.
28. Z. Chen and M. Brookhart, *Acc. Chem. Res.*, 2018, **51**, 1831-1839.
29. D. P. Gates, S. K. Svejda, E. Onate, C. M. Killian, L. K. Johnson, P. S. White and M. Brookhart, *Macromolecules*, 2000, **33**, 2320-2334.
30. D. J. Tempel, L. K. Johnson, R. L. Huff, P. S. White and M. Brookhart, *J. Am. Chem. Soc.*, 2000, **122**, 6686-6700.
31. A. C. Gottfried and M. Brookhart, *Macromolecules*, 2003, **36**, 3085-3100.
32. L. H. Guo, H. Y. Gao, Q. R. Guan, H. B. Hu, J. A. Deng, J. Liu, F. S. Liu and Q. Wu, *Organometallics*, 2012, **31**, 6054-6062.
33. Z. Chen, W. J. Liu, O. Daugulis and M. Brookhart, *J. Am. Chem. Soc.*, 2016, **138**, 16120-16129.
34. S. Mecking, L. K. Johnson, L. Wang and M. Brookhart, *J. Am. Chem. Soc.*, 1998, **120**, 888-899.
35. L. K. Johnson, S. Mecking and M. Brookhart, *J. Am. Chem. Soc.*, 1996, **118**, 267-268.
36. R. López-Fernández, N. Carrera, A. C. Albéniz and P. Espinet, *Organometallics*, 2009, **28**, 4996-5001.
37. P. Xiang and Z. Ye, *J. Organomet. Chem.*, 2015, **798**, 429-436.
38. M. Nagel and A. Sen, *Organometallics*, 2006, **25**, 4722-4724.
39. A. Keyes, H. E. Basbug Alhan, U. Ha, Y.-S. Liu, S. K. Smith, T. S. Teets, D. B. Beezer and E. Harth, *Macromolecules*, 2018, **51**, 7224-7232.
40. W. J. Liu and M. Brookhart, *Organometallics*, 2004, **23**, 6099-6107.
41. L. K. Johnson, C. M. Killian and M. Brookhart, *J. Am. Chem. Soc.*, 1995, **117**, 6414-6415.
42. C. M. Killian, D. J. Tempel, L. K. Johnson and M. Brookhart, *J. Am. Chem. Soc.*, 1996, **118**, 11664-11665.
43. N. Sahloul, A. Emwas, W. Power and A. Penlidis, *Journal of Macromolecular Science, Part A*, 2005, **42**, 1369-1385.
44. G. Moad and D. H. Solomon, in *The Chemistry of Radical Polymerization (Second Edition)*, eds. G. Moad and D. H.

Solomon, Elsevier Science Ltd, Amsterdam, 2005, ch. 4, pp. 167-232.
45. G. Stojcevic, E. M. Prokopchuk and M. C. Baird, *J. Organomet. Chem.*, 2005, **690**, 4349-4355.
46. D. V. Deubel and T. Ziegler, *Organometallics*, 2002, **21**, 4432-4441.
47. M. J. Szabo, R. F. Jordan, A. Michalak, W. E. Piers, T. Weiss, S.-Y. Yang and T. Ziegler, *Organometallics*, 2004, **23**, 5565-5572.
48. B. S. Williams, M. D. Leatherman, P. S. White and M. Brookhart, *J. Am. Chem. Soc.*, 2005, **127**, 5132-5146.
49. C. Fliedel and R. Poli, *J. Organomet. Chem.*, 2018, **880**, 241-252.
50. S. Borkar, D. K. Newsham and A. Sen, *Organometallics*, 2008, **27**, 3331-3334.
51. F. C. Rix, M. Brookhart and P. S. White, *J. Am. Chem. Soc.*, 1996, **118**, 2436-2448.
52. C.-L. Chen, Y.-C. Chen, Y.-H. Liu, S.-M. Peng and S.-T. Liu, *Organometallics*, 2002, **21**, 5382-5385.
53. S. Luo and R. F. Jordan, *J. Am. Chem. Soc.*, 2006, **128**, 12072-12073.
54. S. Luo, J. Vela, G. R. Lief and R. F. Jordan, *J. Am. Chem. Soc.*, 2007, **129**, 8946-8947.
55. M. Cossi and V. Barone, *J. Chem. Phys.*, 2001, **115**, 4708-4717.
56. C. Adamo and V. Barone, *Chem. Phys. Lett.*, 2000, **330**, 152-160.
57. W. Humphrey, A. Dalke and K. Schulten, *J Mol Graph Model*, 1996, **14**, 33-38.
58. A. A. Rusakov, M. J. Frisch and G. E. Scuseria, *J. Chem. Phys.*, 2013, **139**.
59. H. T. Dieck, M. Svoboda and T. Greiser, *Z Naturforsch B*, 1981, **36**, 823-832.
60. K. A. Smoll, W. Kaminsky and K. I. Goldberg, *Organometallics*, 2017, **36**, 1213-1216.
61. P. Huo, T. Chen, J. L. Hou, L. Yu, Q. Y. Zhu and J. Dai, *Inorg. Chem.*, 2016, **55**, 6496-6503.

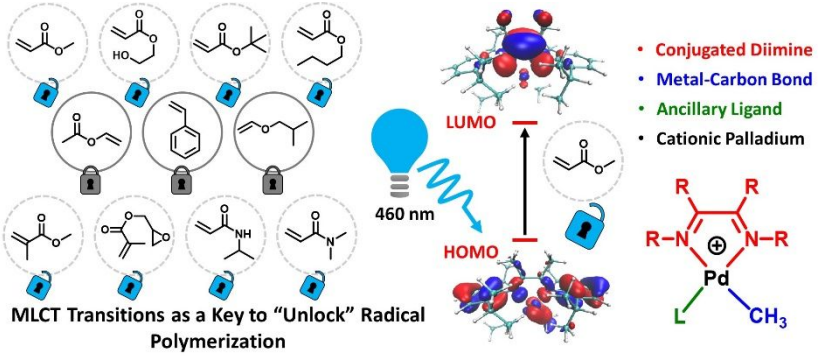

MLCT Transitions as a Key to "Unlock" Radical Polymerization